

# STATUS OF THE DESIGN STUDY FOR 10 MHz POST-ACCELERATED RADIOACTIVE ION BEAMS AT HIE-ISOLDE

M.A. Fraser\*<sup>†</sup>, R. Calaga, CERN, Geneva, Switzerland

## Abstract

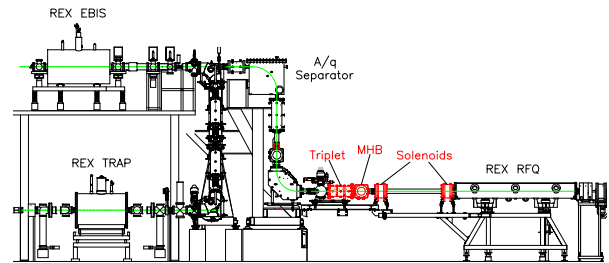
A ten-fold increase in the bunch spacing of post-accelerated radioactive ion beams (RIBs) has been requested by several research groups at ISOLDE, CERN in order for experiments to use time-of-flight particle identification and background suppression techniques. It is proposed to bunch externally into the existing REX (Radioactive ion beam Experiment) RFQ at a sub-harmonic frequency of 10.128 MHz to produce the desired  $\sim 100$  ns bunch separation with minimal loss in transmission. The status of a beam dynamics design study carried out to meet this request will be presented in the framework of the HIE-ISOLDE linac upgrade at CERN.

## INTRODUCTION

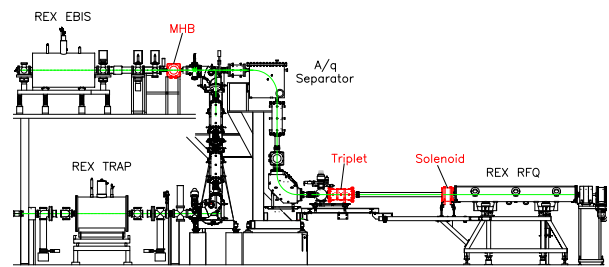
An increased bunch spacing of approximately 100 ns has been requested by several research groups targeting experimental physics at HIE-ISOLDE [1]. It is planned to install a multi-harmonic buncher (MHB) initiating the formation of the longitudinal emittance outside of the RFQ at a sub-harmonic frequency 10 times lower than its 101.28 MHz resonant frequency. This will extend the bunch spacing to 98.7 ns permitting time-of-flight particle identification and background suppression techniques to be used by the experiments. It is foreseen to install the bunching system during the final stage of the HIE-ISOLDE linac upgrade. The layout of the HIE-ISOLDE linac including the bunching and chopping system is shown schematically in Figure 2; more information about the project can be found in [2–4]. The MHB system can be switched off with no impact on the delivery of 101.28 MHz beams.

For low-current applications where space-charge forces are not important, a discrete buncher located either internally or externally to an RFQ accelerator can be used to reduce both the length of the RFQ and the longitudinal emittance [5]. Several nuclear physics accelerator laboratories have employed this design approach, e.g. ANL with the ATLAS upgrade RFQ [6] and TRIUMF with the ISAC RFQ [7]. In most cases the RFQ electrodes are designed without an adiabatic bunching section and an external MHB is placed upstream of the RFQ. In our case we plan to retrofit an existing RFQ that already has electrodes with an adiabatic bunching section. The chosen 10.128 MHz fundamental MHB frequency is similar to the frequencies of both the ANL and TRIUMF systems but the ratio between the RFQ and MHB frequencies is much larger: at HIE-ISOLDE the

ratio is a factor of 10, compared to factors of 5 and 3 for the other systems, respectively. The two different layout options being considered are shown in Figure 1.



(a) A: MHB placed after the REX A/q-separator



(b) B: MHB placed before the REX A/q-separator

Figure 1: Pre-buncher layout options: new components highlighted in red.

## PRE-RFQ BUNCHING

A single-gap, grid-less MHB similar to those employed at ANL and TRIUMF was studied to avoid the transmission losses ( $\sim 20\%$ ) associated with gridded bunchers that are unacceptable for the acceleration of rare RIBs. More details on the optimisation of the MHB electrode geometry can be found in [8]. The feasibility of the MHB-RFQ bunching system at HIE-ISOLDE has been validated with an MHB mixing the first four harmonics of 10.128 MHz. The transmission and rms longitudinal emittance is shown in Figure 3 as a function of the upstream distance ( $L$ ) of the MHB and the effective voltage ( $V_0$ ) of its first harmonic. The iso-contour lines of transmission in Figure 3a indicate that the optimum focal point of the buncher is located 29 cm inside the RFQ at the position on the electrodes where the adiabatic bunching section starts. The longitudinal emittance delivered by the RFQ can be significantly reduced as the drift distance between the RFQ and MHB is increased. Transmissions of up to  $\sim 80\%$  can be expected with  $\sim 15\%$  of the beam spilling out of the main bunch and populating the nine 101.28 MHz satellite bunches, see Figure 4. In

\* The author acknowledges co-funding by the European Commission as a Marie Curie action (Grant agreement PCOFUND-GA-2010-267194) within the Seventh Framework Programme for Research and Technological Development.

<sup>†</sup> mfraser@cern.ch

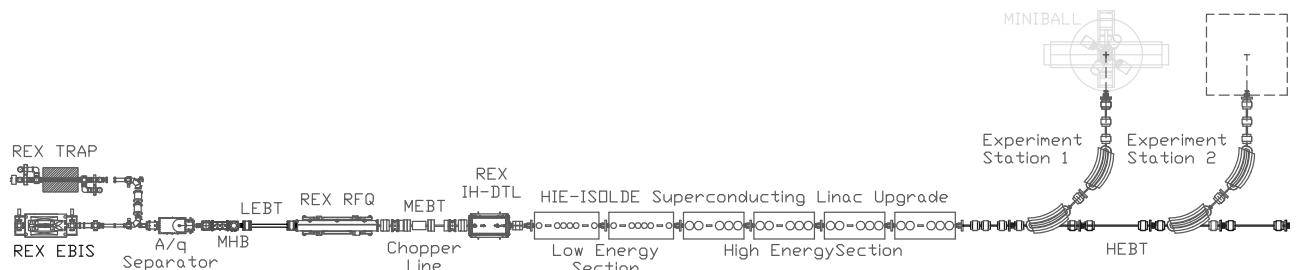
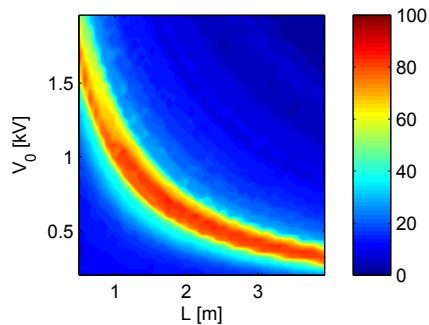
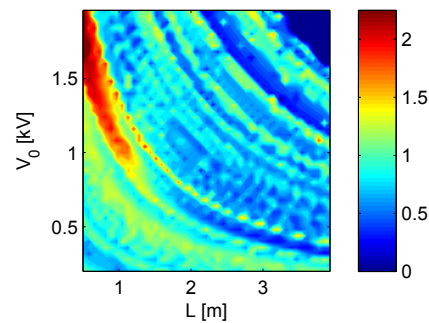


Figure 2: Schematic layout of the HIE-ISOLDE linac installation: MHB, chopper line and 6 superconducting cryomodules.

order to meet the specification requested by the experiments the satellite bunches will need to be removed from the bunch train using a chopper structure placed after the RFQ.



(a) Transmission [%] after RFQ.



(b) Longitudinal emittance: ratio with dc injection,  $\epsilon_{MHB}^{rms} / \epsilon_{dc}^{rms}$ .

Figure 3: Survey of  $L$  and  $V_0$  for a four-harmonic MHB.

## BEAM DYNAMICS STUDIES

In order to characterise the beam dynamics in the Low Energy Beam Transfer (LEBT) line between the EBIS and RFQ, the entire system was simulated by tracking particles through the 3D field maps of each active component, including the RFQ [9], using the TRACK code [10]. The tracking simulations were matched using a COSY- $\infty$  model [11] that incorporated fringe field effects and a benchmarking of the two codes showed that Taylor maps computed to third-order were adequate to describe the non-linear transverse beam dynamics [12]. TRACK was required for a complete understanding of the non-linear longitudinal dynamics in the LEBT and RFQ. The results of the study are summarised in Table 1.

The study identified geometric aberrations induced by the existing electrostatic quadrupoles before the RFQ as a source of emittance growth. This motivated the design of a new LEBT employing solenoids, which is more tolerant to the increase in energy spread introduced by the MHB because the beam size can be kept compact in both orthogonal phase space planes. In addition, this helps to minimise the non-isochronous effects that introduce phase-lagging and cause the bunch length to increase at the focal point inside the RFQ.

The MHB can also improve beam purity by time-of-flight filtering of nearby  $A/q$  contaminants into the satellite bunches, which are chopped and thus removed from the bunch train [13].

### Option A

Option A provides a relatively simple integration solution with the MHB placed directly before the RFQ. However, large voltages must be applied to the electrostatic triplet to realise a beam waist in the MHB and as a result geometric aberrations cause transverse emittance growth. The beam size in the triplet is large because of the tight waist made at the mass selection slit in the upstream diagnostic box directly after the separator. This option is flexible should the MHB need moving closer to the RFQ; an increased beam energy spread is expected from a proposed upgrade of the EBIS [14]. The effect of a large (order of magnitude) increase in the beam energy spread from the ion source was simulated with the MHB located just 0.9 m before the RFQ. The results are collected as option C in Table 1. An increased beam energy spread from the EBIS limits the performance of the system.

### Option B

The large drift distance between the MHB and RFQ in option B provides a solution that offers a significant reduction of the longitudinal emittance. The MHB is placed at a position on the beam line after the ion source that will require careful integration into a crowded region. The  $A/q$ -separator is not completely achromatic and as a consequence a small amount of transverse emittance growth occurs in the vertical plane where the dispersion function is non-zero downstream. Nonetheless, the emittance growth is less than that induced by the aberrations of option A. In addition, the time-of-flight filtering by the bunching system would increase the resolution of the existing mass separator by a factor of  $\sim 3$ .

Table 1: Summary of the simulated beam dynamics performance of the different MHB layout options

| Upgrade Option | MHB Status | $V_0^a$ [V] | $L$ [m] | $\frac{\Delta A/q}{A/q}$ | $\Delta\phi^b$ [deg] | $\frac{\Delta W}{W}$ source [%] | $T_{\text{total}}$ [%] | $T_{10 \text{ MHz}}$ [%] | $T_{\text{sat}}$ [%] | $\epsilon_{x,\text{rms}}, \epsilon_{y,\text{rms}}$ [mm mrad] | $\epsilon_{z,\text{rms}}$ [ns keV/u] |
|----------------|------------|-------------|---------|--------------------------|----------------------|---------------------------------|------------------------|--------------------------|----------------------|--|--------------------------------------|
| A              | ON         | 465         | 2.32    | $\sim \frac{1}{150}$     | -30                  | 0.1                             | 98.6                   | 82.4                     | 16.2                 | 0.93, 0.72   | 0.15                                 |
|                | OFF        | 0           |         | -                        | -                    | 0.1                             | 94.3                   | -                        | -                    | 0.95, 0.74   | 0.26                                 |
| B              | ON         | 175         | 9.49    | $\sim \frac{1}{500}$     | -70                  | 0.1                             | 98.5                   | 83.2                     | 15.3                 | 0.70, 0.79   | 0.08                                 |
|                | OFF        | 0           |         | -                        | -                    | 0.1                             | 93.9                   | -                        | -                    | 0.60, 0.63   | 0.27                                 |
| C              | ON         | 1150        | 0.87    | -                        | -30                  | 1.0                             | 76.9                   | 54.2                     | 22.7                 | 0.74, 0.76   | 0.59                                 |
|                | OFF        | 0           |         | -                        | -                    | 1.0                             | 93.4                   | -                        | -                    | 0.72, 0.78   | 0.27                                 |

<sup>a</sup> The effective voltage experienced by the beam:  $V_{\text{eff}} = V_0 (\sin \omega_0 t - 0.43 \sin 2\omega_0 t + 0.21 \sin 3\omega_0 t - 0.10 \sin 4\omega_0 t)$ .

<sup>b</sup> RFQ phase shift relative to MHB at 101.28 MHz to compensate for the phase-lagging of non-isochronous particles.

### Error Studies

Rf error studies were performed in order to specify the stability of the voltage and phase of the MHB [8]. The phase jitter of the MHB must be an order of magnitude better than the RFQ because of the large ratio between the fundamental frequencies of the two structures, i.e. the effect of jitter on the beam at 10.128 MHz is amplified by a factor of 10 after the RFQ. The studies showed a significant increase in the time-averaged rms longitudinal emittance for a jitter of  $\sigma_\phi > 0.1$  deg. at 10.128 MHz and  $\sigma_V > 0.5\%$ .

### POST-RFQ CHOPPING

In principle, chopping could take place before the RFQ. However, this was discounted because of the need to ‘grid’ the chopper plates and the concomitant loss of transmission; the aperture is far larger than the permitted longitudinal extent of the chopper fields, which must be  $\ll \beta\lambda_{\text{MHB}} = 97$  mm. The feasibility of cleanly removing the satellite bunches from the bunch train with a travelling-wave type chopper placed after the RFQ was demonstrated using a quasi-static model comprising a chain of synchronised capacitors pulsed at high-voltage [15]. The travelling-wave option was preferred over a two-frequency resonant chopper, e.g. the ISAC system at TRIUMF [16], because the proximity of the satellite bunches ( $\beta\lambda_{\text{RFQ}} = 75$  mm) demands shorter electrodes, and consequently larger voltages, to avoid significantly perturbing the main 10.128 MHz bunches. The power requirements of the structure are less of a concern because of the duty factor ( $< 10\%$ ) of the injector. In addition, the travelling-wave chopper can be programmed to remove an arbitrary number of 10.128 MHz pulses to extend even further the dead-time. A classic chopper line design is employed in the Medium Energy Beam Transfer (MEBT) line [4] demanding 4 mrad of deflection from the chopper, which can be kept shorter than 0.5 m with a voltage of 1.2 kV. The MEBT maintains the acceptance of the machine whilst the predicted transverse emittance growth is negligible provided the rise/fall time of the chopper is  $< 5$  ns. The specification of the chopper is similar to the double meander strip-line chopper developed at CERN for Linac4 [17]. Although the

chopper would require scaling to match the beam velocity after the REX RFQ ( $\beta = 0.0254$ ), the demands on the power amplifiers in terms of burst repetition rate ( $< 50$  Hz), burst length ( $< 2$  ms), pulse rise/fall time ( $< 5$  ns), pulse length ( $\sim 90$  ns) and voltage ( $\pm 0.6$  kV) are also similar.

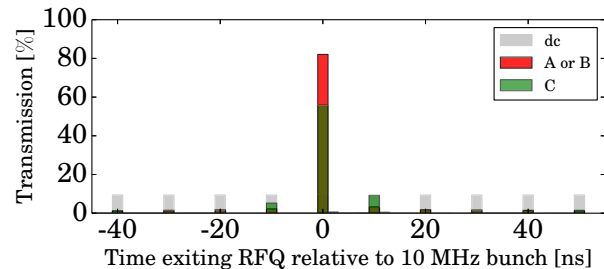


Figure 4: Bunch intensity distribution at the RFQ exit. Results for options A and B are similar and plotted together.

### CONCLUSION

A beam dynamics design study has been completed for a bunching system that can provide optional 10 MHz post-accelerated RIBs to the ISOLDE user community at CERN.

### ACKNOWLEDGMENT

We acknowledge funding from the Swedish Knut and Alice Wallenberg Foundation (KAW 2005-0121) and from the Belgian Big Science program of the FWO (Research Foundation Flanders) and the Research Council K.U. Leuven. The authors would also like to thank Martin Berz (MSU) for advice on implementing fringe fields in COSY- $\infty$  and Brahim Mustapha (ANL) for his help with the TRACK simulations.

## REFERENCES

- [1] S.J. Freeman *et al.*, CERN-INTC-2010-031, CERN (2010).
- [2] W. Venturini Delsolaro *et al.*, THIOA03, these proceedings.
- [3] M.A. Fraser *et al.*, HIAT'12, Chicago, WEC02 (2012) 175.
- [4] M.A. Fraser *et al.*, IPAC'13, Shanghai, THPWO076 (2013) 3933.
- [5] J. Staples, *Part. Accel.* 47 (1994) 191.
- [6] P. N. Ostroumov *et al.*, *Phys. Rev. ST Accel. Beams* **15** (2012) 110101.
- [7] S. Koscielniak *et al.*, LINAC'96, Geneva, TUP32 (1996) 402.
- [8] M.A. Fraser, CERN-HIE-ISOLDE-PROJECT-Note-0035, CERN, to be published.
- [9] M.A. Fraser, R. Calaga, CERN-ACC-NOTE-2014-0015, CERN (2013).
- [10] TRACK: <http://www.phy.anl.gov/atlas/TRACK>
- [11] COSY INFINITY: <http://bt.pa.msu.edu/cosy>
- [12] M.A. Fraser, D. Voulot and F. Wenander, CERN-ACC-NOTE-2014-0017, CERN (2013).
- [13] M. Marchetto, HIAT'12, Chicago, MOC01 (2012) 33.
- [14] A. Shornikov *et al.*, *Nucl. Instrum. Meth. B* **317** (2013) 395.
- [15] A. Mukhopadhyay, M.A. Fraser *et al.*, CERN-ACC-NOTE-2014-0016, CERN (2013).
- [16] R.E. Laxdal *et al.*, LINAC'02, Gyeongju, TU441 (2002) 407.
- [17] F. Caspers, T. Kroyer and M. Paoluzzi, CERN-AB-Note-2008-040 RF, CARE/HIPPI Document - 2008-20, CERN (2008).